JETIR.ORG ISSN: 2349-5162 | ESTD Year : 2014 | Monthly Issue
JOURNAL OF EMERGING TECHNOLOGIES AND INNOVATIVE RESEARCH (JETIR)
An International Scholarly Open Access, Peer-reviewed, Refereed Journal

COMPARATIVE ANALYSIS OF LSTM AND ARIMA MODELS FOR PREDICTING AEROSOL OPTICAL DEPTH IN LUCKNOW AND DELHI CITIES

Zaid Ahmad[1], Amarendra Singh[2], Saumya Singh[3], Prabhat Kumar Patel[4]

[1] M.Tech Student, [2] Assistant Professor, [3] Assistant Professor, [4]Assistant Professor

[1,2,3,4] Department of Civil Engineering, Institute of Engineering and Technology, Lucknow Uttar Pradesh- 226021, India

Abstract: The aim of this research is to compare the accuracy of predictive models using Aerosol Optical Depth (AOD) for the cities of Delhi and Lucknow. We applied both Long Short-Term Memory (LSTM) and Auto Regressive Integrated Moving Average (ARIMA) models for AOD prediction for January 2023 using past 10 years data (i.e., 01-01-2013 to 01-01-2023) in both locations in order to accurately analyse their performances. It is observed that ARIMA model (in both cases) performs better than LSTM model and have better accuracy in predicting. The ARIMA models exhibited lower Mean Squared Error (MSE) and Root Mean Squared Error (RMSE) values (i.e., Lucknow - MSE: 0.01843, RMSE: 0.1357; Delhi - MSE: 0.03672, RMSE: 0.1916) along with lower Mean Absolute Percentage Error (MAPE) values (i.e., Lucknow - 18.9975%; Delhi - 20.80004%). Furthermore, the ARIMA models showed higher R-Square values (i.e., R^2: Delhi - 0.5994, Lucknow - 0.7335;) compared to the LSTM models (i.e., R^2: Lucknow - 0.5452, Delhi - 0.5590). The study gives valuable insights into the spatial variability of AOD and underscores the significance of employing ARIMA models for time series prediction in regions characterized by distinct AOD patterns. To evaluate air quality as well as mitigate environmental effects, it is essential to comprehend these aerosol patterns.
Keywords: Aerosol optical depth; LSTM; ARIMA; Lucknow; Delhi.

1. Introduction:

Aerosols, often referred to as particulate matter, originate from both human activities and natural sources. They are known to have detrimental impacts on both atmospheric contamination and human welfare (Al-Kindi et al., 2020, Burnett et al., 2018). Elevated stages of air pollutants, like aerosols, are related with various health problems, including lung cancer, respiratory diseases, and heart issues (Russell et al., 2009, Davidson et al., 2005). Furthermore, atmospheric aerosols can affect our Earth's heat balance (Srivastava et al., 2022, Haywood et al., 2000).

AOD is a measure of how much solar radiation is absorbed or scattered by aerosols throughout the entire atmospheric column, providing insights into aerosol concentrations. There are two primary approaches to measuring AOD namely satellite-based and ground-oriented remote detection. In comparison to satellite measurements, ground-oriented methods offer simplicity and fairly higher accuracy [Wu et al., 2015, Lin et al., 2013]. AOD serves as a crucial optical property parameter for characterizing aerosol optical characteristics. It holds particular significance due to its high precision in measurement and the wide range of observational methods available [Xue et al., 2017].

Over the last twenty years, many research projects have looked at how aerosols are spread, what they look like, and how they move in specific areas of South of Asia, especially in the Indo-Gangetic Plain (IGP). These studies have used a combination of computer simulations and actual data collection (M. G. Lawrence et al.,2010, M. A. Bollasina et al.,2011, V.S.Nair et al.,2012, V.Vinoj et al.,2014, Shi et al., 2016, Shahid et al.,2020).

Several models have been settled on the basis of satellite results for the evaluation of AOD. Though, the models are influenced by the quality of AOD product recoveries and uncertainties associated with other factors (Shunlin Liang et al.,2006; F. Melin et al.,2007; Ling Gao et al.,2016; E.Sun et al.,2019). Improved accuracy in AOD retrieval has been achieved through new artificial intelligence (AI) methods. Artificial neural network (ANN) models have been constructed to recover AOD at both global and regional gauges (A. Ali et al.,2013; Wenmin Qin et al.,2018). Additionally, for long sequential time series of Moderate Resolution Imaging Spectroradiometer (MODIS), integrating

Support Vector Machine (SVM) and ANN yielded poor AOD estimates compared to MODIS AOD products (Bethania Lanzaco et al.,2017).

To address the extensive issue of air pollution, it's essential to create effective and practical prediction models. Numerous studies have explored air quality prediction, and various researchers have proposed different methods. These diverse approaches collectively enhance the accuracy of predicting air quality (Jun Luo et.al 2023). The LSTM algorithm was first introduced in (Sepp Hochreiter et al.,1997). It has demonstrated successful results in various fields, particularly in handling sequential time problems, like rainfall and overflow simulations (Frederik Kratzert et al.,2018; Caihong Hu et al.,2018; Hanlin Yin et al.,2021), stock prediction (D. M. Nelson et al.,2017), language modelling (Y. Li et al.,2018), machine translations (I. Sutskever et al.,2014), and speech understanding (A. Graves et al.,2013). Based on the previously mentioned research, the LSTM approach is highly recommended for addressing time sequential problems.

In recent times, and especially over the last few decades, weather forecasting models have seen extensive use in research by numerous scientists. Among these models, the ARIMA model have emerged as one utmost fit for understanding climatic variables, such as precipitation and temperature. These models have been found to be effective and reliable in capturing the patterns and variations in these important climate factors (Tripti Dimri et al.,2020).

Despite extensive research on air quality patterns using different network models, there is a absence of complete studies comparing performance of models like LSTM and ARIMA. To address this gap, this study will analyze AOD levels in Lucknow and Delhi cities over a 10-year period. The data used for this research is obtained from NASA's Giovanni platform, specifically from the MODIS Terra satellite.

Moreover, this investigation will employ LSTM and ARIMA network models to foresee future AOD levels for both cities. By linking the presentation of these models, the study intent to ascertain the most suitable forecasting method for AOD in Lucknow and Delhi.

2. Data and Methods:

2.1 Description and meteorology of the site

This research is based upon two urban cities, Lucknow and Delhi, both situated in the Uttar Pradesh state of India and experiencing a steppe climate. The study focuses to examine the difference of predictive capability of LSTM and ARIMA modelling techniques by using AOD values of these highly developed places. Both cities experience extreme weather conditions, with very hot summers reaching up to 45°C and cold winters where temperatures can drop as low as 3°C.

More about selected area is discussed below:

2.1.1 Lucknow

Lucknow is located in the central IGP in north of India at a latitude about 26.84°N and longitude about 80.94 °E. Its elevation is approximately 128 meters above mean sea level. It is situated along the picturesque banks of the Gomti River. Identified for its rich artistic legacy and historic importance, the metropolitan is shelter to a significant population density (about 40 lakhs according to World Population Review based on latest revised UN World Urbanization Prospects). City spans an area of 349 square kilometres with its increasing population, there are about 8,100 people living in every square kilometre. However, Lucknow faces environmental issues, particularly concerning air and water pollution, due to its high population and rapid urbanization (i.e., Ring roads and metro construction).

This growth, combined with an approximately 10% rise in the number of vehicles on the road each year, has resulted in a significant increase in registered motor vehicles. According to data from the Regional Transport Office (RTO), the number of registered vehicles went up from 11 lakhs in 2010 to 24 lakhs in 2017.

When examining the factors responsible for overall air pollution in Lucknow, it becomes evident that the main culprits are vehicle emissions and the dust stirred up from roads by vehicles and ongoing metro construction.

2.1.2 Delhi

Delhi is set in the north-western part of the IGP at a latitude about 28.39°N and longitude about 77.09°E, have an elevation around 215 meters above mean of sea level. It is a densely populated city with approximately 1.7 crores people based upon Census of 2011. It extents to an area of about 1500 km^2. Delhi is enclosed by the Himalayan mountains in the north, the flatlands of centre part of India to the south, and the Thar Desert in the west-southwest. In the nearby areas of Delhi, you can find many small and medium-sized factories, and they add to the pollution. Also, Delhi has around 71 lakhs registered vehicles, and these are the main reasons for the contaminated air in the region.

The special geographical features of the IGP, with the Himalayan mountains to the north, trap various aerosols in the area. This situation worsens air pollution in both cities.

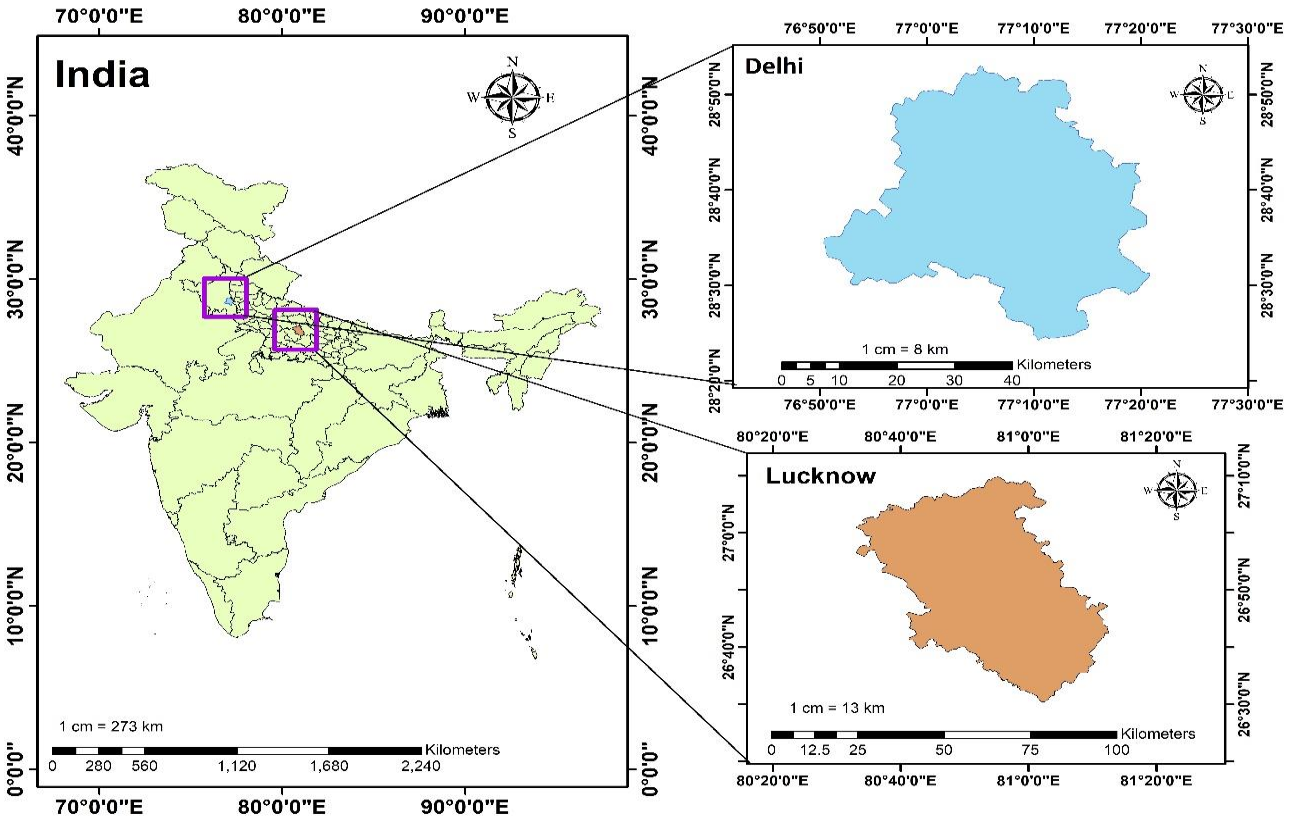

Fig.1 Area location map of Lucknow and Delhi cities within India.

2.2 Data collection

In our study, we collected AOD statistics at 1-degree daily resolution from January 1, 2013, to January 1, 2023, for both cities. We obtained this data from NASA's MODIS Terra platform, specifically using the dataset known as MODIS-Terra MYD08_D3 v6.1. We retrieved the data from NASA's GIOVANNI website.

MODIS, is an imperative tool on NASA's Terra and Aqua satellites. Both of these spacecrafts were sent out in 1999 and 2002, respectively. MODIS helps us gather extensive data about the Earth's atmosphere, land, and oceans, which is crucial for Earth research.

One remarkable feature of MODIS is its ability to provide data at different levels of detail, ranging from 250 meters to 1 kilometre, depending on the type of information needed. This wide range allows scientists to study various aspects of our planet with great accuracy.

What's even better is that MODIS data is available to the public and can be accessed through various platforms, like NASA's EOSDIS. This open accessibility promotes transparency and encourages scientists from around the world to use this valuable information for a wide range of research and applications.

2.3 Methodology

2.3.1 LSTM

As mentioned earlier, the LSTM algorithm was first introduced in (Sepp Hochreiter et al.,1997) and this algorithm is based upon Recurrent Neural Network (RNN) (Rumelhart et al. 1986).

The diagram below illustrates four neural network layers represented by green boxes, point-wise operators denoted by white circles, input shown in blue circles, and the cell state represented by yellow circles. An LSTM module consists of a cubicle (cell) state and 3 gates, granting it the ability to learn selectively, unlearn, or hold info from individual unit. The cell state facilitates the movement of information from the components while limiting alterations, allowing only a few linear interactions.

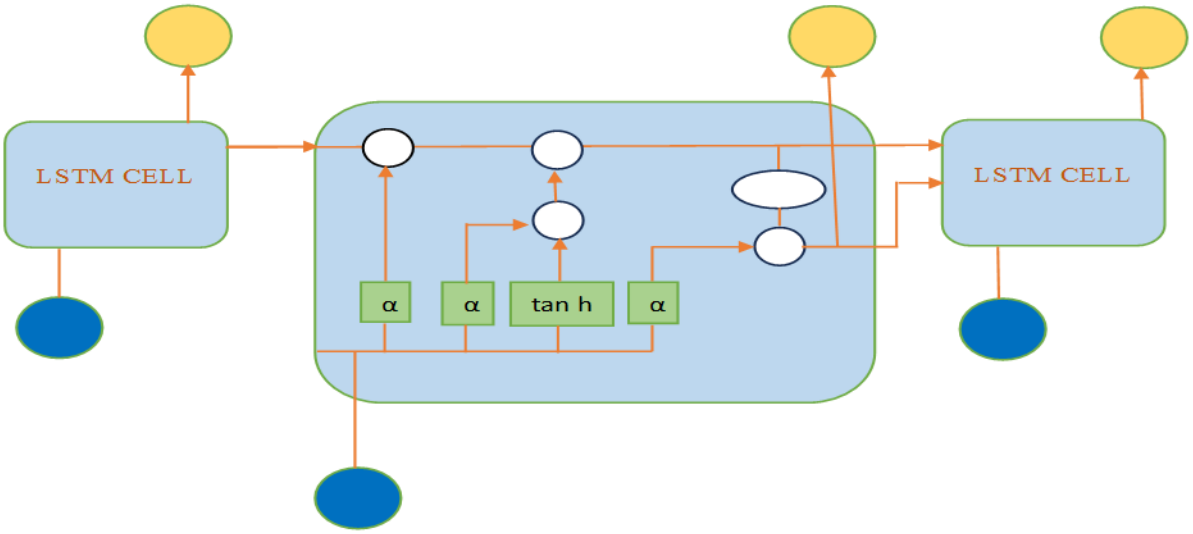

Fig.2. LSTM network flow diagram.

An individual LSTM unit comprises 3 gates namely an input gate that retains available info, an output gate that regains the output, and a forget gate that discards or ignores historical data by using the sigmoid function. The input gate regulates the movement of information into the present cell state by utilizing a point-wise duplication procedure involving 'sigmoid' and 'tanh'. Subsequently, the output gate determines which data should be transmitted to the following concealed state. (Eltahan et al.2020).

2.3.2 ARIMA

The standard abbreviation for a non-seasonal ARIMA model is ARIMA (p, d, q), where p denotes the lag order, d the order of differencing, and q the order of the moving average. A seasonal ARIMA model, on the other hand, is denoted by the notation ARIMA (p, d, q) (P, D, Q) m, where m is the number of periods in each season. For the seasonal component of the ARIMA model, the letters P, D, and Q stand for the respective moving average (MA), differencing (I), and autoregressive (AR) factors. (Tripti Dimri et al.,2020). All the three models together make ARIMA model.

Although ARIMA procedure has restrictions as it relies on past values, it can work well for extended and unchanging time series data. However, it only approximates historical trends rather than offering an explanation of the core data mechanism (Balibey and Serpil 2015; Bari et al. 2015; Yoosef Doost et al. 2017). Since, the data is stationary, a non-seasonal ARIMA model has been used. We performed the time series analysis as described in the flow chart below:

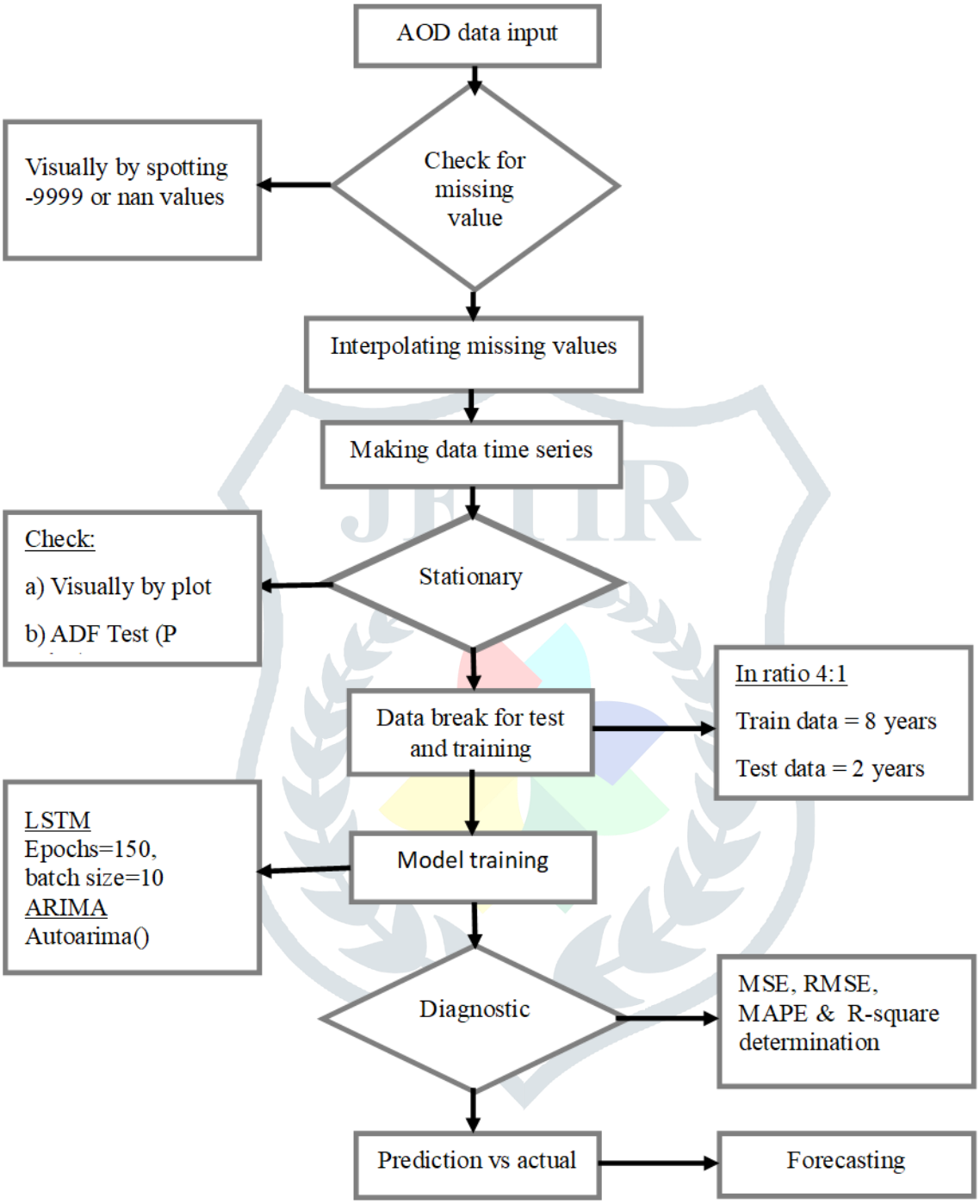

Fig.3. Flow chart of time series analysis using LSTM and ARIMA network models.

Initially, we checked for missing values in AOD data and found many by inspection so we carried out forward and backward interpolation to fill those missing values. Usually, the missing values are dropped in python but since data had so many missing values, so interpolation method was chosen for better results. After that the data is converted in time series format to carry out our analysis.

To check whether the AOD data is stationary we did visual inspection and also ADF (Augmented Dickey-Fuller) test which is an arithmetical method used to govern the stationarity of a time series data, examining whether it possesses a

unit root (non-stationary) or not, and is conducted to identify trends and patterns in the data for time series analysis. We have used python for ADF test to determine the stationarity of the data.

After that the data was broken into test and train data in 4:1. Firstly, we have used a LSTM neuronal network model for time series estimating and trained it to get prediction done using python, it also gave the plots between actual vs predicted data for both the cities and the forecasted AOD values for next month. The LSTM architecture is compatible for catching long-standing dependence and outlines in chronological data like time series. Here's a description of the model:

(a) Model Architecture:

The model contains numerous layers, individually serving a definite purpose.

The first LSTM layer has 512 memory units, and it processes the input data while maintaining the sequence of time steps (`return sequences=True`). It learns patterns and dependencies across the time steps in the input data.

After the first LSTM layer, a dropout layer is added to prevent overfitting. 20% of the neurons are randomly neutralised via dropout during training, which lessens the model's reliance on any one neuron and enhances generalisation. The second LSTM layer has 256 memory units and also processes the input with the same sequence retention (`return_sequences=True`).

Another dropout layer is included after the second LSTM layer to further regularize the model.

The third LSTM layer has 128 memory units. Unlike the previous layers, it only returns the last output, as `return_sequences` is not specified here. This layer helps capture higher-level temporal patterns in the data.

A dropout layer is applied again after the third LSTM layer to enhance the model's robustness against overfitting.

Two fully allied (dense) layers are included at the end of the model. The first dense layer contains 64 units and helps the model learn more abstract representations of the data. The second dense layer has only one unit and serves as the output layer, predicting the next value in the time series.

(b) Model Compilation:

The model is prepared for training using the `compile()` method.

The Mean Squared Error (MSE) loss function is chosen as it is appropriate for regression tasks like time series forecasting. The model aims to minimalize the difference amongst its calculations and the authentic target values.

The RMSprop optimizer is employed to optimize the model's weights during training. It adjusts with the learning frequency founded on the magnitude of recent gradients.

The learning frequency is established to 0.001, which governs the step size for weight updates throughout training.

(c) Model Training:

The model is accomplished on the provided time series data by means of the `fit()` method.

The training statistics, consisting of arrangements of entered features (`X_train`), and the equivalent target values (`Y_train`) are fed into the model during training.

The training process is repeated for 150 epochs, meaning the model goes through the entire training dataset 150 times. This allows the model to learn from the data in multiple passes, refining its ability to make accurate predictions.

To update the model's weights after processing a small batch of data, a batch size of 10 is used. This efficient training technique helps speed up the training process while maintaining accurate learning updates.

In summary, the model is a deep LSTM neural network designed to arrest composite temporal patterns in time series data. It is trained to minimize the mean squared error and make accurate predictions for future values in the time series.

Similarly ARIMA model autoarima() is used in R- studio which itself chooses the best fit values for p,d and q was used to get the same plots. The monthly AOD values are used here instead of daily. The performance of both LSTM and ARIMA models is checked with respect to MSE, RMSE, MAPE & R-square values and finally the comparison between LSTM and ARIMA model is made on the same.

The provided code uses the ARIMA model for time series forecasting. Here's a concise explanation of the code:

(a) `model <- auto.arima(ts_data)`: The code fits ARIMA model to `ts_data` time series by means of the `auto.arima()` function, which itself chooses the finest ARIMA model founded on certain criteria, and the resulting model is stored in the variable `model`.

(b) `forecast_data <- forecast(model, h = 30)`: The code generates forecasts for the future 30 time periods using the `forecast()` function with the previously fitted ARIMA model (`model`). The forecasted data is stored in the variable `forecast_data`.

(c)`best_model <- auto.arima(train_data)`: The code finds the finest ARIMA model for `train_data` time series using the `auto.arima()` function. The selected model is stored in the variable `best_model`.

(d)`forecast_data <- forecast(best_model, h = length(test_data))`: The code generates forecasts for the same time period as the actual data using the previously identified best ARIMA model (`best_model`). The number of future time periods to forecast is set to the length of the test data. The projected data is stored in the variable `forecast_data`.

In summary, the code uses the `auto.arima()` function to find the best ARIMA model for the provided time series data. It then generates forecasts for future time periods using this model and also forecasts for the same time period as the actual data. The ARIMA model is useful for making predictions in time series analysis.

3.Results and discussion

3.1 ADF Test: Since we have used python for ADF test to determine the stationarity of the data for both the cities, we got following values:

Table. 1: P-values and significance level found applying ADF-test.

SI No.	Location	P values	Significance level
1.	Lucknow	$2.5741e-^{12}$	0.05
2.	Delhi	$1.6443e-^{13}$	0.05

- First p-value: $1.644355158430538e-^{13}$ (approximately 1.64×10^{-13} or 0.000000000000164).
- Second p-value: $2.5741638537063304e-^{12}$ (approximately 2.57×10^{-12} or 0.00000000000257).

Both p-values are extremely small, indicating strong evidence against the null hypothesis of non-stationarity. The null hypothesis may be rejected because both p-values are significantly below the usual significance level of 0.05, which allows us to draw the conclusion that the data is stationary. It's great that we obtained consistent results from the ADF test in both cases, confirming the stationarity of the time series data. This suggests that the data exhibits stable statistical properties over time, making it suitable for time series analysis and forecasting.

3.2 Time series analysis:

Firstly, the plot between predicted and actual values of AOD using LSTM network model is shown in which a comparison can be seen in from 01-01-2022 to 01-01-2023 for the both the cities (i.e., Lucknow at left and Delhi at right hand side).

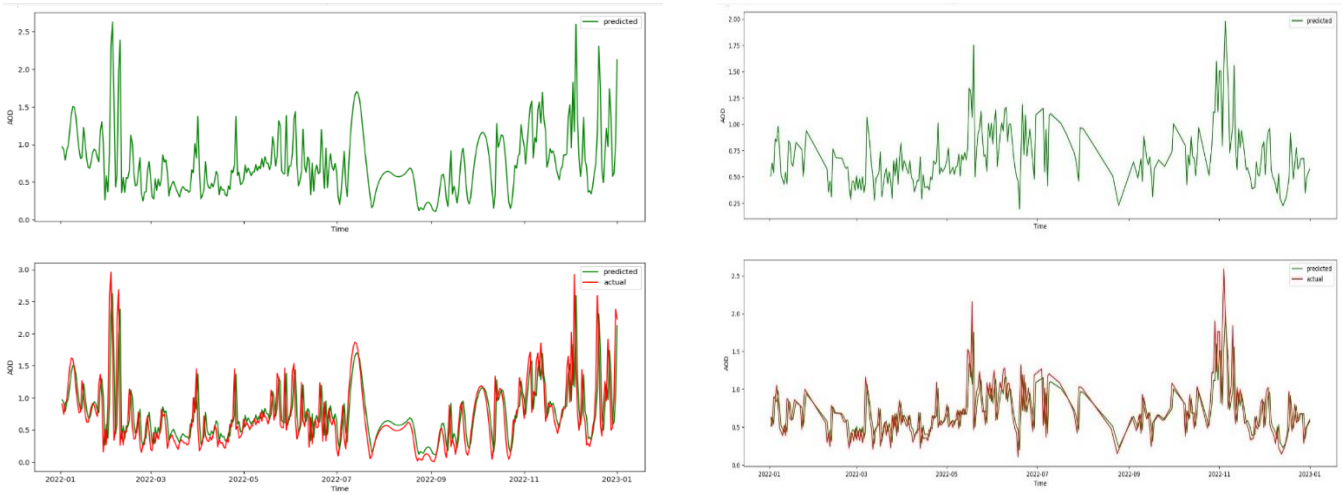

Fig.4. Predicted vs actual AOD values diagram for Lucknow (left) and Delhi (right) city using python.

Similarly, after that the plot future forecasted values using same LSTM model for next month (i.e., Jan 2023) is shown for both the cities.

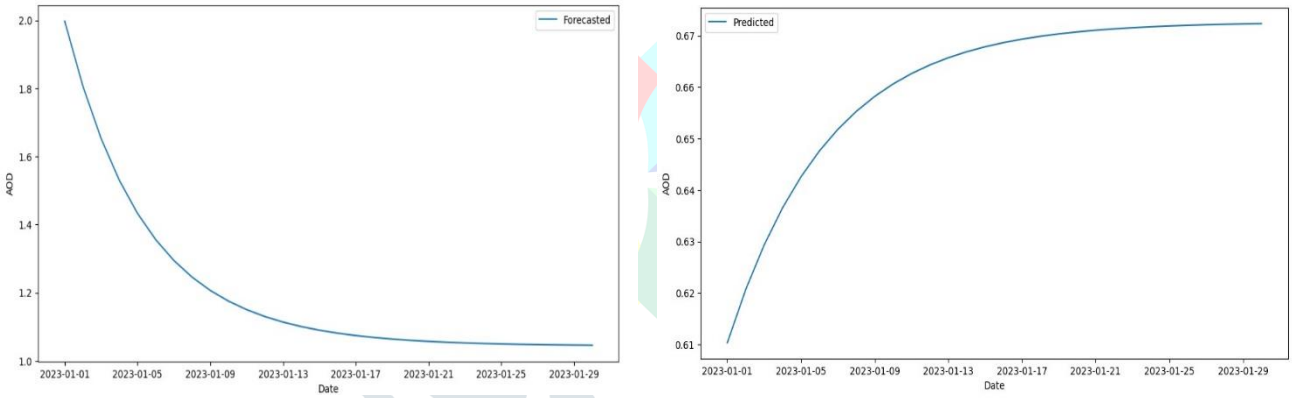

Fig.5. Predicted (forecasted) AOD values diagram for Lucknow (left) and Delhi (right) cities for January 2023 using LSTM model

In January 2023, using an LSTM model, we forecasted the Aerosol Optical Depth (AOD) for Delhi and Lucknow cities on a daily basis. The predicted AOD values for Delhi extended from 0.610 to 0.672, while for Lucknow, the AOD values were greater, ranging from 1.543 to 1.927.

Delhi generally experienced lower AOD values compared to Lucknow throughout the month, indicating that Delhi had relatively cleaner air with fewer aerosols in the troposphere. On the other hand, Lucknow had higher AOD values, suggesting higher concentrations of aerosols, which can lead to reduced visibility and potential health impacts, especially for individuals with respiratory conditions.

Similarly, the plot between predicted and actual values of AOD using ARIMA model on R-studio is shown in which a comparison can be seen in from 2022 to 2023 for the both the cities (i.e Delhi on left and Lucknow at right hand side).

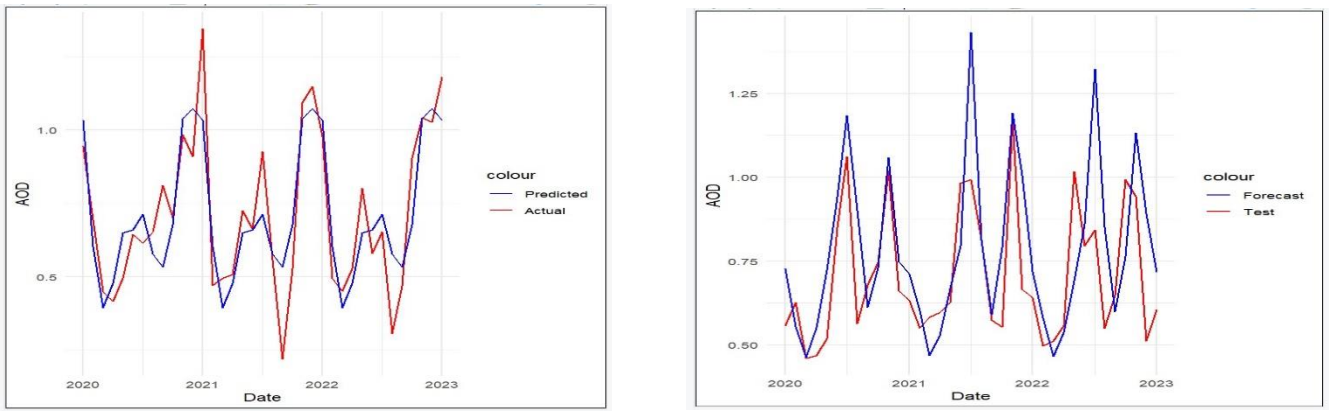

Fig.6. Predicted vs actual AOD values diagram for Lucknow (left) and Delhi (right) city using R-studio.

After that the plot future forecasted values using same ARIMA model for next month (i.e Jan 2023) is shown for both the cities.

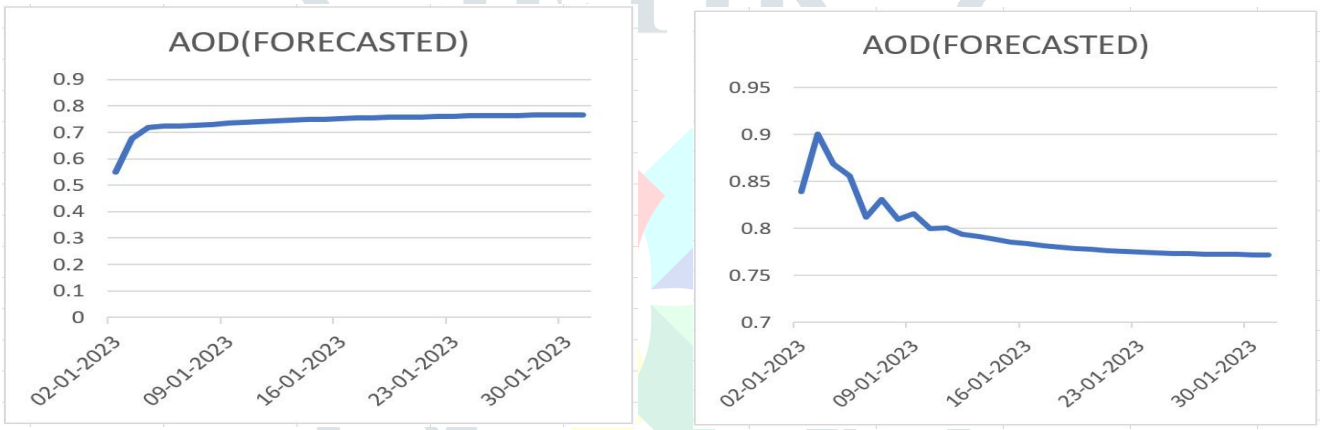

Fig.7. Predicted (forecasted) AOD values diagram for Lucknow (left) and Delhi (right) cities for January 2023 using ARIMA model.

In January 2023, using the ARIMA model, Lucknow's forecasted Aerosol Optical Depth (AOD) exhibited a consistent pattern with a gradual increase over the month. The AOD standards fluctuated from 0.550 to 0.766. This gradual increase in AOD indicates an upward trend in aerosol concentrations in Lucknow's atmosphere, which can be associated with worsening air quality and reduced visibility.

On the other hand, Delhi's AOD values ranged from 0.839 to 0.771 and showed fluctuations during the month. While Delhi experienced varying AOD levels, the overall trend appeared to be a decrease in aerosol concentrations from greater values at the opening of the month to lower values towards the end of January. This trend may suggest potential improvement in air quality and visibility over the course of the month.

Both cities should closely monitor AOD levels as they provide valuable information about air contamination and its potential influence on human well-being and the environment. It is vital to implement required air quality management measures in order to solve the difficulties presented by aerosol concentrations while also guaranteeing a healthy living environment for their population.

3.3 Models comparison:

Table. 2: Errors and R^2 standards for LSTM and ARIMA models:

SI No.	Location	Model name	MSE	RMSE	MAPE (%)	R-Square
1.	Lucknow	LSTM	0.1412	0.3758	54.0076	0.5452
2.	Lucknow	ARIMA	0.01843	0.1357	18.9975	0.7335
3.	Delhi	LSTM	0.06161	0.2482	26.1785	0.5590
4.	Delhi	ARIMA	0.03672	0.1916	20.80004	0.5994

The assessment of the LSTM and ARIMA models employed for both cities is given in Table 2 using MSE, RMSE, MAPE, and R-Square values.

In this investigation, we calculated how well the LSTM and ARIMA models performed at predicting data from two separate locations, Lucknow and Delhi. The assessment was based on the MSE, Root RMSE, MAPE, and R-Square (R2) metrics.

In Delhi, both the LSTM and ARIMA models displayed reasonable predictive capabilities. In terms of MSE, RMSE, and MAPE, the ARIMA model outperformed the LSTM model. The ARIMA model produced more accurate predictions with fewer mistakes thanks to reduced MSE and RMSE values. The ARIMA model also displayed a lower MAPE indicating that its forecasts were more accurate. The ARIMA model's R-Square value was also greater, indicating a better fit of the model to the statistics and more variance being clarified.

The Lucknow dataset indicated comparable tendencies. On the basis of MSE, RMSE, and MAPE, the ARIMA model outperformed the LSTM model suggestively. The ARIMA's lower MSE and RMSE figures demonstrated its capacity to generate more accurate forecasts with fewer errors. Additionally, the ARIMA model showed a lower MAPE, which demonstrated its capacity to produce predictions that were more in line with the actual data. Additionally, the ARIMA model's greater R-Square value demonstrated a better fit to the data, implying that it captured more volatility in the target variable.

Overall, according to the evaluation measures, both in Lucknow and Delhi, the ARIMA models outperformed the LSTM models in terms of predictive performance.

4.Conclusions:

Both the LSTM and ARIMA models for predictive modelling were assessed for data prediction in Delhi and Lucknow. In terms of MSE, RMSE, MAPE, and R-Square for both sites, the ARIMA models outperformed the LSTM models, demonstrating superior prediction accuracy and model fit. For these particular time series prediction tasks, the ARIMA models might be thought of as being more appropriate. However, it's vital to know that the success of a model also rest on the explicit characteristics of the dataset and the nature of the problem being addressed. These results emphasize the potential usefulness of ARIMA models for time series prediction tasks in these locations. This could help to conduct further analysis and experimentation to explore other modelling approaches and enhance predictive accuracy in these regions.

Acknowledgements:

I would like to express my appreciation to the Civil Engineering Department at IET Lucknow for their ongoing support and guidance as I used Python to do research on AOD and its variations in the cities of Delhi and Lucknow. The knowledge of Python and Arc GIS was of great help to me in completing my assignment. I'm grateful to NASA's GIOVANNI webpage for easily giving me access to AOD data.

References:

[1] Al-Kindi, S. G., Brook, R. D., Biswal, S., & Rajagopalan, S. (2020). Environmental determinants of cardiovascular disease: Lessons learned from air pollution. *Nature Reviews. Cardiology, 17*, 656–672.

[2] Burnett, R., et al. (2018). Global estimates of mortality associated with long-term exposure to outdoor fine particulate matter. *Proceedings of the National Academy of Sciences of the United States of America, 115*, 9592.

[3] Russel, A. G., & Brunekreef, B. (2009). A Focus on Particulate Matter and Health. *Environmental Science & Technology, 43*(13), 4620–4625. doi:10.1021/es9005459.

[4] Davidson, L., Borg, M., Mann, I., Topor, A., Mezzina, R., & Sells, D. (2005). Processes of Recovery in Serious Mental Illness: Findings from a Multinational Study. *American Journal of Psychiatric Rehabilitation, 8*(3), 177–201.
[5] Srivastava, N., Saini, S. A., & Shukla, S. (2022). Aerosol optical depth in various seasons, using MODIS data - A study of Lucknow district. *International Research Journal of Engineering and Technology (IRJET), 09*(04), 804-809.
[6] Haywood, J., & Boucher, O. (2000). Estimates of the direct and indirect radiative forcing due to tropospheric aerosols: A review. *Reviews of Geophysics, 38*(4), 513-543.
[7] Wu, Y. F., Zhu, J., Che, H. Z., Xia, X. G., & Zhang, R. J. (2015). Column-integrated aerosol optical properties and direct radiative forcing based on sun photometer measurements at a semi-arid rural site in Northeast China. *Atmospheric Research, 157*, 56–65.
[8] Lin, H. F., Xin, J. Y., Zhang, W. Y., Wang, Y. S., Liu, Z. R., & Chen, C. L. (2013). Comparison of atmospheric particulate matter and aerosol optical depth in Beijing City. *Environmental Science, 34*, 826–834.
[9] Xue, Y., He, X. W., de Leeuw, G., Mei, L. L., Che, Y. H., Rippin, W., ... & Hu, Y. C. (2017). Long-time series aerosol optical depth retrieval from AVHRR data over land in North China and Central Europe. *Remote Sensing of Environment, 198*, 471–489.
[10] Lawrence, M. G., & Lelieveld, J. (2010). Atmospheric pollutant outflow from southern Asia: a review. *Atmospheric Chemistry and Physics, 10*(22), 11017–11096. https://doi.org/10.5194/acp-10-11017-2010
[11] Bollasina, M. A., Ming, Y., & Ramaswamy, V. (2011). Anthropogenic Aerosols and the Weakening of the South Asian Summer Monsoon. *Science, 334*(6055), 502-505. https://doi.org/10.1126/science.1204994
[12] Nair, V. S., Solmon, F., Giorgi, F., Mariotti, L., Babu, S. S., & Moorthy, K. K. (2012). Simulation of South Asian aerosols for regional climate studies. *Journal of Geophysical Research: Atmospheres, 117, D04209. doi:10.1029/2011JD016711.
[13] Vinoj, V., & Rasch, P., & Wang, H., & Yoon, J. H., & Ma, P. L., & Kiranmayi, & Landu, & Singh, B. (2014). Short-term modulation of Indian summer monsoon rainfall by West Asian dust. *Nature Geoscience, advance online publication*, 308–313.
[14] Shi, H., Wang, Y., Chen, J., & Huisingh, D. (2016). Preventing smog crises in China and globally. *Journal of Cleaner Production, 112*, 1261–1271.
[15] Shahid, M. Z., Shahid, I., & Zahid, M. (2020). Inter-annual variability and distribution of aerosols during winters and aerosol optical thickness over Northeastern Pakistan. *International Journal of Environmental Science and Technology, 19*, 875–888.
[16] Liang, S., Zhong, B., & Fang, H. (2006). Improved estimation of aerosol optical depth from MODIS imagery over land surfaces. *Remote Sensing of Environment, 104*(4), 416–425.
[17] M´elin, F., Zibordi, G., & Djavidnia, S. (2007). Development and validation of a technique for merging satellite-derived aerosol optical depth from SeaWiFS and MODIS. *Remote Sensing of Environment, 108*(4), 436–450.
[18] Gao, L., Li, J., Chen, L., Zhang, L., & Heidinger, A. K. (2016). Retrieval and validation of atmospheric aerosol optical depth from AVHRR over China. *IEEE Transactions on Geoscience and Remote Sensing, 54*(11), 6280–6291.
[19] Sun, E., Che, H., Xu, X., Wang, Z., Lu, C., Gui, K., ... & Wang, Y. (2019). Variation in MERRA-2 aerosol optical depth over the Yangtze River delta from 1980 to 2016. *Theoretical and Applied Climatology, 136*(1-2), 363–375.
[20] Ali, A., Amin, S. E., & Ramadan, H. H. (2013). Enhancement of OMI aerosol optical depth data assimilation using artificial neural network. *Neural Computing and Applications, 23*(8), 2267–2279. https://doi.org/10.1007/s00521-012-1178-9.
[21] Qin, W., Wang, L., Lin, A., Zhang, M., & Bilal, M. (2018). Improving the Estimation of Daily Aerosol Optical Depth and Aerosol Radiative Effect Using an Optimized Artificial Neural Network. *Remote Sensing, 10*(7), 1022. https://doi.org/10.3390/rs10071022

[22] Lanzaco, B., & Olcese, L. (2017). An Improved Aerosol Optical Depth Map Based on Machine-Learning and MODIS Data: Development and Application in South America. *Aerosol and Air Quality Research, 17*, 1523-1536.
[23] Luo, J., & Gong, Y. (2023). Air pollutant prediction based on ARIMA-WOA-LSTM model. *Department of Ocean Engineering Equipment, Zhejiang Ocean University, Zhoushan, 316022, China*.
[24] Hochreiter, S., & Schmidhuber, J. (1997). Long Short-Term Memory. *Neural Computation, 9*(8), 1735–1780. doi: https://doi.org/10.1162/neco.1997.9.8.1735.
[25] Kratzert, F., Klotz, D., Brenner, C., Schulz, K., & Herrnegger, M. (2018). Rainfall–runoff modeling using long short-term memory (LSTM) networks. *Hydrology and Earth System Sciences, 22*(11), 6005–6022.
[26] Hu, C., Wu, Q., Li, H., Jian, S., Li, N., & Lou, Z. (2018). Deep Learning with a Long Short-Term Memory Networks Approach for Rainfall-Runoff Simulation. *Water, 10*, 1543. https://doi.org/10.3390/w10111543.
[27] Yin, H., Wang, F., Zhang, X., Zhang, Y., Chen, J., Xia, R., & Jin, J. (2022). Rainfall-runoff modeling using LSTM-based multi-state-vector sequence-to-sequence model. *Journal of Hydrology, 610*, 127901. https://doi.org/10.1016/j.jhydrol.2022.127901
[28] Nelson, D. M., Pereira, A. M., & Oliveira, R. A. (2017). Stock market's price movement prediction with LSTM neural networks. In *2017 International Joint Conference on Neural Networks (IJCNN)* (pp. 1419-1426).
[29] Li, Y., & Cao, H. (2018). Prediction for Tourism Flow based on LSTM Neural Network. *Procedia Computer Science, 129*, 277-283. https://doi.org/10.1016/j.procs.2018.03.076.
[30] Sutskever, I., Vinyals, O., & Le, Q. V. (2014). Sequence to sequence learning with neural networks. In *Advances in neural information processing systems* (pp. 3104–3112).

[31] Graves, A., Mohamed, A. -r., & Hinton, G. (2013). Speech recognition with deep recurrent neural networks. In *2013 IEEE International Conference on Acoustics, Speech and Signal Processing* (pp. 6645-6649). doi: 10.1109/ICASSP.2013.6638947
[32] Kuj, T., Ahmad, S., & Sharif, M. (2020). Time series analysis of climate variables using seasonal ARIMA approach. *Journal of Earth System Science, 129*, 149. https://doi.org/10.1007/s12040-020-01408-x.
[33] Rumelhart, D., Hinton, G., & Williams, R. (1986). Learning representations by back-propagating errors. *Nature, 323*, 533–536. https://doi.org/10.1038/323533a0
[34] Eltahan, M., & Moharm, K. (2020). Atmospheric Aerosol Prediction over Egypt with LSTM-RNN using NASA's MERRA-2. In *2020 International Conference on New Trends in Information & Communications Technology Applications (NTICT)* (pp. 93-98). doi: 10.1109/NILES50944.2020.9257885.
[35] Balibey, M., & Türkyilmaz, S. (2015). A time series approach for precipitation in Turkey. *Environmental Earth Sciences, 28*, 549-559.
[36] Bari, S. H., Rahman, M. T. U., Hussain, M. M., & Ray, S. (2015). Forecasting Monthly Precipitation in Sylhet City Using ARIMA Model. *Civil and Environmental Research, 7*, 69-77.
[37] Yoosefdoost, A., Sadeghian, M., Nodefarahani, M., & Rasekhi, A. (2017). Comparison between Performance of Statistical and Low-Cost ARIMA Model with GFDL, CM2.1, and CGM 3 Atmosphere-Ocean General Circulation Models in Assessment of the Effects of Climate Change on Temperature and Precipitation in Taleghan Basin. *American Journal of Water Resources, 5*, 92-99. https://doi.org/10.12691/ajwr-5-4-1